Monticeli, Francisco M.; Neves, Roberta M.; Ornaghi, Heitor L.; Almeida, Humberto

A systematic review on high-performance fiber-reinforced 3D printed thermoset composites

Published in:
Polymer Composites

DOI:
10.1002/pc.26133

Published: 01/08/2021

Received: 14 March 2021 | Revised: 3 May 2021 | Accepted: 7 May 2021
DOI: 10.1002/pc.26133

REVIEW ARTICLE

spe INSPIRING PLASTICS PROFESSIONALS Polymer COMPOSITES WILEY

A systematic review on high-performance fiber-reinforced 3D printed thermoset composites

Francisco M. Monticeli[1] | **Roberta M. Neves**[2] | **Heitor L. Ornaghi Jr**[3] | **José Humberto S. Almeida Jr**[4,5]

[1]Department of Materials and Technology, São Paulo State University, Guaratinguetá, São Paulo, Brazil
[2]PPGE3M, Federal University of Rio Grande do Sul, Porto Alegre, Rio Grande do Sul, Brazil
[3]Materials Engineering, Federal University for Latin American Integration (UNILA), Foz do Iguaçu, Paraná, Brazil
[4]Department of Mechanical Engineering, Aalto University, Espoo, Finland
[5]Advanced Composites Research Group, School of Mechanical and Aerospace Engineering, Queen's University Belfast, Belfast, UK

Correspondence
José Humberto S. Almeida Jr, Department of Mechanical Engineering, Aalto University, Espoo, Finland.
Email: humberto.almeida@aalto.fi

Funding information
Royal Academy of Engineering, Grant/Award Number: RF\201920\19\150

Abstract
High-performance fiber-reinforced thermoset composites processed by additive manufacturing (3D printing) are attracting substantial attention in both academic and industrial fields in a market currently dominated by thermoplastic matrices. Thermoset polymers have, nevertheless, several advantages over thermoplastic ones. This study aims at recommending suitable fibers and processing conditions that effectively improve the mechanical properties of thermoset composites produced by additive manufacturing. The influence of void content is also highlighted. A systematic review is performed here using the Preferred Reporting Items for Systematic Reviews and Meta-Analyses (P.R.I.S.M.A.) protocol as a guide aiming to identify the main findings recently studied. A total of 147 studies are initially identified within 2014–2020 using three scientific databases. Then, 29 articles are selected and described respecting several inclusion and exclusion criteria. The main findings are presented and discussed, and the gaps are identified to open up further investigations yet to be understood and exploited.

KEYWORDS
additive manufacturing, composites, thermosets

1 | INTRODUCTION

There is no doubt that additive manufacturing (AM) revolutionized the manufacturing field especially given the possibility to produce complex geometries with inexpensive equipment requirements.[1,2] Thus, the number of works and companies dealing with such AM composites keeps increasing. It is well known that polymeric matrices in composites are either thermoplastic or thermoset, and thermoset-base composites are far more disseminated than thermoset ones.[3] The majority of works found in literature use thermoplastic matrices since such materials have the advantage of easy temperature control, the reuse filament possibility, equipment cleaning, and maintenance, more precise control of material sizing, among others.[4–7]

Thermoset matrices usually have higher strength than thermoplastics, and they are more used in high-end structural applications because they do not melt like thermoplastics.[8–11] However, there is a considerable difficulty in controlling viscosity for deposition and curing the printed material, maintaining its complex three-dimensional geometry–an essential factor for AM.[12,13] As a response, a significant number of studies have been developed aiming at improving the processability, such as the optimal set of printing speed/thickness, printing direction, thermoset matrix, and fiber used, AM type, among others.[14–16]

Thermoset matrices application through AM relies on a new horizon in terms of efficiently processing parts and components with the advantages of possessing suitable mechanical properties while having complex geometries and little tooling.[17,18] This processing ensures an appropriate reinforcement/matrix interfacial impregnation since both materials are extruded together. However, there is still a difficulty in impregnation control to reduce defects such as void formation due to the high complexity of the processing factors – compared with traditional infusion processing methods (e.g., resin transfer molding [RTM], hand lay-up, resin film infusion [RFI]).[19–23] An important advantage of thermoset is that the adhesion increases between the printed filaments since the shear stress becomes a limiting factor due to the lower load capacity of thermoplastics, which have mainly secondary bonding between filaments.[24]

Considering different literature studies, some questions are still unanswered, such as the optimal AM processes used, the mechanical/thermal behavior regarding the process applied, and the main challenges in AM of thermoset fiber-reinforced polymers (FRP). Aiming at fulfilling these gaps and answer previous questions, this work proposes a systematic review focusing on fiber-reinforced thermoset composites processed by AM. The systematic review protocol herein undertaken is based on recently published papers.[25,26] The contribution to the field is a systematic review approach of process parameter-mechanical/thermal behavior, the shortcoming identification and gaps in the literature, and the presentation of a reference document for future research.

2 | ADDITIVE MANUFACTURING OF FIBER-REINFORCED POLYMER COMPOSITES

The processing type is defined according to reinforcement (i.e., continuous, short, or milled fibers) and matrix since the procedure will depend on selecting the material.[27] Thermoset composite processing parameters are determined using kinetic energy, usually measured using differential scanning calorimetry (DSC).[28,29] Among others, Borchardt and Daniels, Kissinger, and Barrett methods consider the energy involved in the process as an extension of functional group consumption (α).[29] Considering the need for quick curing after the filament deposition, the widest resins used are those with an injection/cure temperature $< 100^\circ$C with a short cure time.[30–32]

Another usual factor in ensuring the impregnation quality is the viscosity, which influences the infusion parameters, void formation, and material geometry, and ensures an appropriate fiber/matrix interface.[13] Viscosity is directly proportional to temperature, in which the vibration of the molecules increases the monomers distance and decreases the shear stresses resistance.[33] The viscosity for AM presents values 10–100 fold higher than the conventional injection processes, which occurs mainly due to two factors: (i) addition of short fibers mixed with epoxy matrix, which increases the viscosity[34]; and (ii) geometry maintenance after filament deposition,[20,35] or otherwise, it would be necessary to print onto a rigid mold.

Ming et al.[16] show the possibility of complex structure manufacturing of carbon fiber reinforced thermoset composite (Figure 1), in which pentagram and honeycomb structures (Figures 1(A),(B)) present no naked-eye visible resin-rich regions, interlayer delamination, and low void content (Figures 1(C),(D)). The possibility of processing complex structures, such as honeycomb structure, allows the application of high specific stiffness in new structural components, which is difficult to achieve with conventional composite manufacturing methods.[16,36]

Both mechanical and physical properties synergy of the thermoset matrix combined with carbon fiber are responsible for the high specific stiffness of structural composites. Figure 2 presents a comparative analysis of the mechanical properties against the density of conventional metals and FRP thermoset composite processed by AM.[17] As expected, high fiber fractions (V_f) significantly increase the strength of the composite. Nawafleh et al.[17] demonstrate that weight reduction represents about 85% compared with conventional steel (Steel 4140 annealed and Steel 1040 hot rolled) and about 45% of aluminum components (Al 6061/2024) and similar properties. As a matter of fact, 27% of short fibers present the mechanical behavior close to Al 6061 and Steel 1040 hot rolled. In addition, a composite with 46% of short fibers shows similar strength compared with Al 2024 and Steel 4140 annealed.

The fiber size (short, long, continuous) is also an important factor that contributes to mechanical properties, in which the increase in fiber size is directly proportional to the increase in mechanical strength until a limit that there is sufficient matrix to evolve and keep the fibers at their original orientation.[17,20] Another issue is also associated with fiber dispersion and impregnation homogenization.[37,38] Figure 3 shows the influence of fiber content on AM quality (via stereolithography printer–Figure 3(A)). The increase of glass fiber powder could result in inappropriate composite impregnation (Figure 3(B)), which increases defects formation and decreases the mechanical behavior. On the other hand, the use of low volume fraction (i.e., 10 wt%) enables a complex component additive manufacturing (Figure 3 (C)), establishing the challenge of optimizing the AM

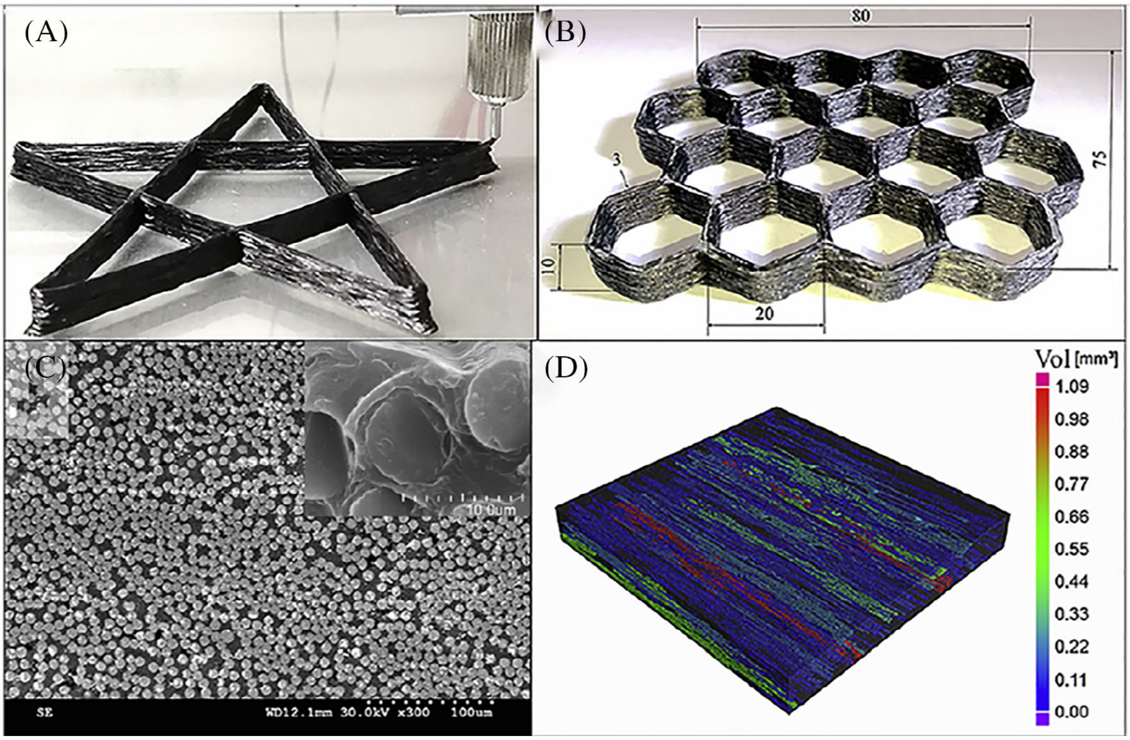

FIGURE 1 Additive manufacturing (A) pentagram structure, (B) honeycomb structure, and the corresponding (C) cross-sectional scanning electron microscopy, and (D) internal structures after curing (using micro CT)[16]–with permission of Elsevier [Color figure can be viewed at wileyonlinelibrary.com]

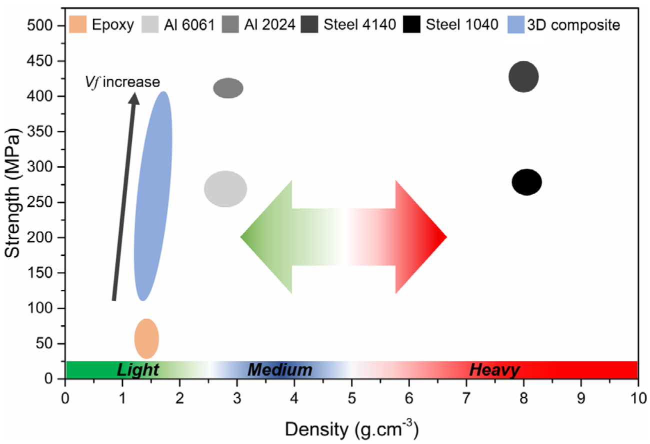

FIGURE 2 Comparison of mechanical behavior against density variation of AM thermoset composites and metals (based on References [17]) [Color figure can be viewed at wileyonlinelibrary.com]

process for high fiber content, suitable for structural applications.[36]

Based on Shi et al.,[12] Sanei et al.[27], and Van de Werken et al.,[7,39] Figure 4 exhibits the mechanical property variation associated with the fiber size and the working temperature based on the glass transition temperature (T_g) of the matrix. As previously mentioned, the increase in fiber size increases the mechanical behavior; meanwhile, the working temperature is governed mainly by the matrix (thermoplastic or thermoset). The thermoset matrices allow the material application at higher glass transition due to the strong molecular cross-link interaction compared with thermoplastic matrices used for AM.[12]

The fiber size used also limits the AM method to be employed, in which the fused filament fabrication (FFF) and localized in-plane thermal assisted (LITA) present methods of impregnating long fibrous reinforcement.[12,32] On the other hand, direct ink writing (DIW) and stereolithography (SLA) processing are useful for short fibers.[15,36] AM composites aim to achieve similar properties as those produced via conventional manufacturing processes with high fiber volume fraction and low defects.[12,36] Hot isostatic processing (HIP) was only found for thermoplastic carbon fiber/PEEK composite, not yet explored for thermoset 3D printed composites.[7]

In addition to conventional process control procedures, such as temperature control, viscosity, and impregnation behavior, AM should also consider aspects such as print speed, curing pressure, infill density/pattern, and fiber volume fractions to ensure that the print filaments present suitable viscosity for injection and quick cure after deposition. Thus, it is possible to ensure the resin flow during printing, low void content, strong fiber-resin interface, and good mechanical and thermal behavior.[16,30]

Mechanical and thermal responses are directly affected by (i) the AM method used[40]; (ii) reinforcement

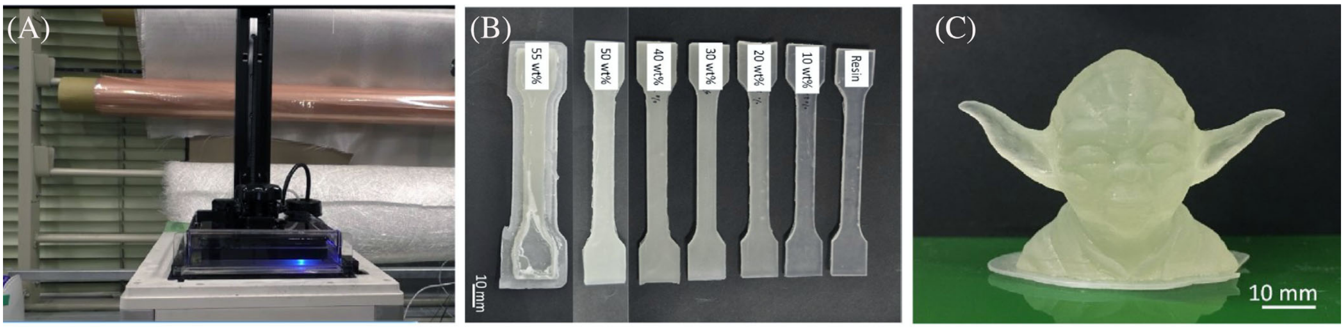

FIGURE 3 (A) Stereolithography printer method, (B) test specimen of glass fiber powder composites printed by stereolithography, and (C) complex figure printed from 10 wt% glass fiber powder composites[36]–With permission of Elsevier [Color figure can be viewed at wileyonlinelibrary.com]

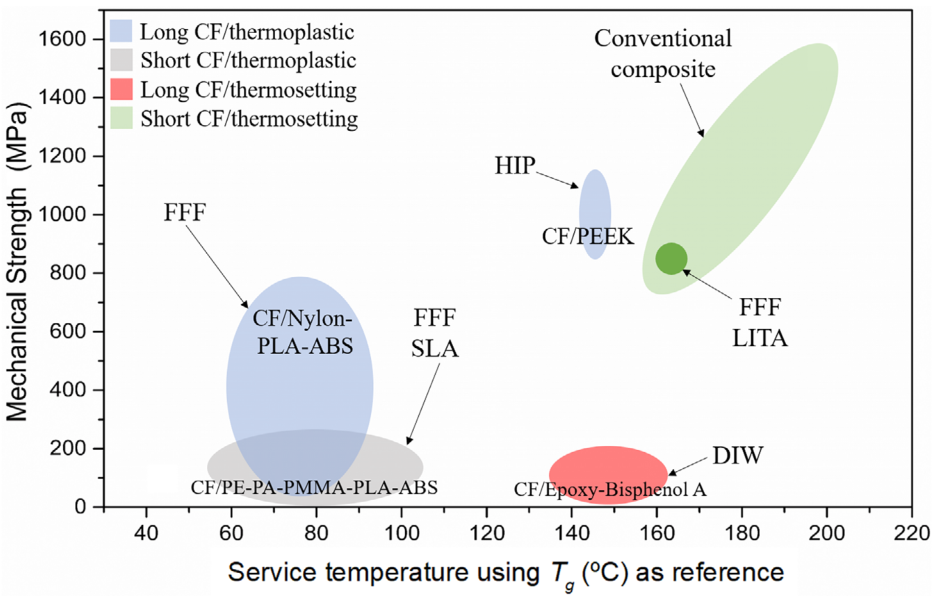

FIGURE 4 Comparison of mechanical strength and glass transition (T_g) of 3D-printed composites regarding fiber size, matrix system, and processing method (based on References [12]). ABS, acrylonitrile butadiene styrene; CF, carbon fiber; FFF, fused filament fabrication; SLA, stereolithography, DIW, direct ink writing, LITA, located in-plane thermal assisted; HIP, hot isostatic processing; PEEK, poly-ether-ether-ketone; PE, polyethylene; PA, polyamide; PMMA, poly(methyl methacrylate); PLA, polylactide [Color figure can be viewed at wileyonlinelibrary.com]

type: the extrusion process usually sort of provides a preferred orientation to short fibers aided by the extrusion direction, which increases their mechanical performance[41]; (iii) matrix system associated with reinforcement interaction, processing control, and toughness behavior[24]; and (iv) the response of processing factors that could generate impregnation defects, such as voids, affect the final properties.[14] Considering the wide combination of factors that generates a variation on the quality and properties of FRP thermoset composite processed by AM, the systematic review carried out here allows a scientific contribution for a complete analysis of the literature along with highly reliable results analysis.

3 | SYSTEMATIC REVIEW METHODOLOGY

A systematic review is defined as research that uses the literature as a source of data, providing a summary of the evidence related to a specific intervention strategy by applying explicit and systematic methods of search, critical evaluation, and information synthesis about a specific topic.[25,27]

Preferred Reporting Items for Systematic Reviews and Meta-Analyses (P.R.I.S.M.A.) guidelines are followed for conducting this review.[25] Three different databases from the literature were selected (Scopus–www.scopus.com, Web of Science–www.webofknowledge.com, and Mendeley–www.mendeley.com), regarding search papers focused on the studies in thermoset composites processed by AM approaches. For the search, the following terms are used: ([thermoset] AND [composite] AND [3D] AND [printing] OR [additive] AND [manufacturing] [fiber] AND {[glass] OR [carbon] OR [Kevlar]}). The search was done from 2014 to 2020.

The AM process type, process parameters, and reinforcement are analyzed through the studies following the

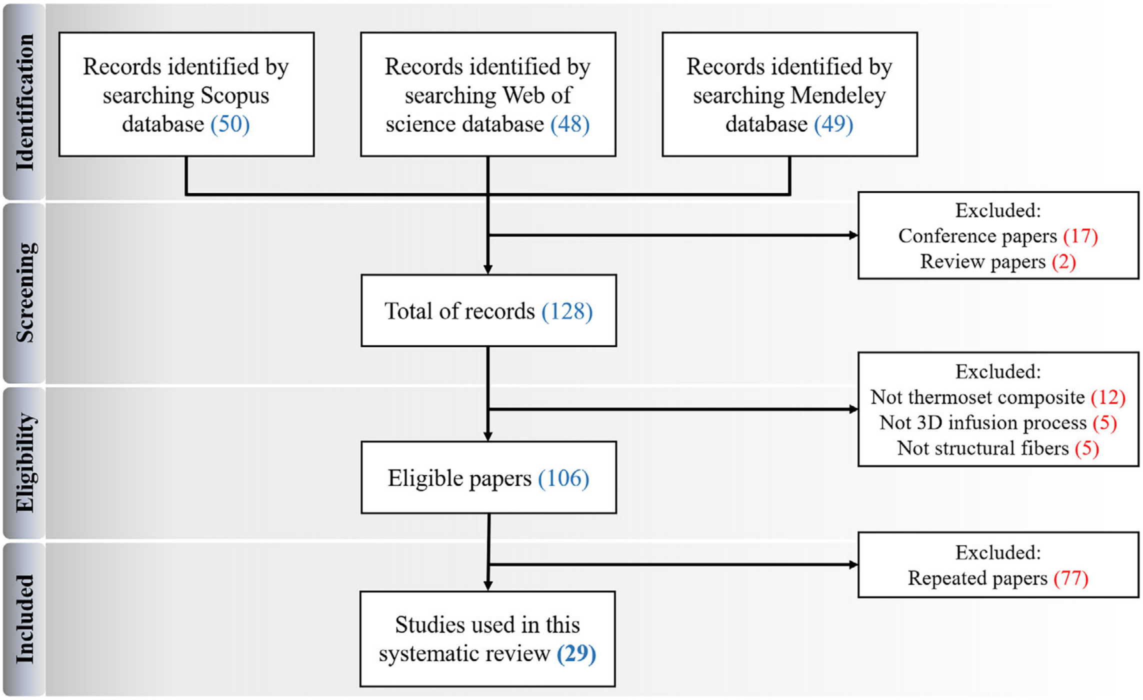

FIGURE 5 Search and selection process diagram, following P.R.I.S.M.A. protocol[25] [Color figure can be viewed at wileyonlinelibrary.com]

void formation, mechanical, and thermal/dynamic mechanical properties.

4 | DATA COLLECTION RESULTS

Figure 5 shows the search and selection process diagram, following P.R.I.S.M.A. protocol,[25,26] which includes identification, screening, eligibility, and included steps. The identification resulted in 147 papers, including all research types, following the specific terms aforementioned. For the second step, the first exclusion process is performed, in which conference and review papers are not considered, resulting in 128 papers. At the eligibility step, the removed papers are those with no thermoset composite (11)–for instance, papers that use thermoplastic composites for thermoset composite repair, processed by conventional methods; not an AM process (5)–e.g., thermoplastic mold associated with handing lay-up thermoset composite processing; and not use structural fiber (5)–e.g., natural fibers, resulting in 107 papers. The final process is the included paper, in which repeated papers are excluded. In the end, 29 papers are eligible and therefore selected for the present work.

5 | RESULTS AND DISCUSSION

Figure 6 presents the AM paper frequency in the literature for papers included in the current methodology. Figure 6(A) shows the frequency of papers published over the years (2014–2020) from a broad field perspective. There is an increasing trend in the subject since the topic is undoubtedly under development and still in the early stages to reach enough maturity for generating high-quality structural components.

Figure 6(B) shows the main tests performed through studies in literature, in which the mechanical test is the most applied, being both bending and tensile tests the most utilized, but fatigue, impact, and shear tests have also been performed at a lower frequency. Thermal tests are only considered after the processing since it is always performed before printing to ensure the process parameters. The main analysis is thermogravimetry and dynamical mechanical analysis, but at a lower frequency than mechanical tests. Thus, the lack in the literature is highlighted, and the possibilities for new studies in thermal analysis of AM thermoset composites.

Void measurement is also performed (Figure 6(B)). Voids are mainly characterized using optical and scanning electron microscopy and X-ray microtomography, considering the possibility to measure void content, morphology, and location. A distinct void characterization is used for the AM process: pore inside the printed section and void formation space between the printed section.[14,16] Nevertheless, authors consider every space inside or between printed filament as the total void content,[12,20,34] which is more in accordance with the usual porosity definition.[42]

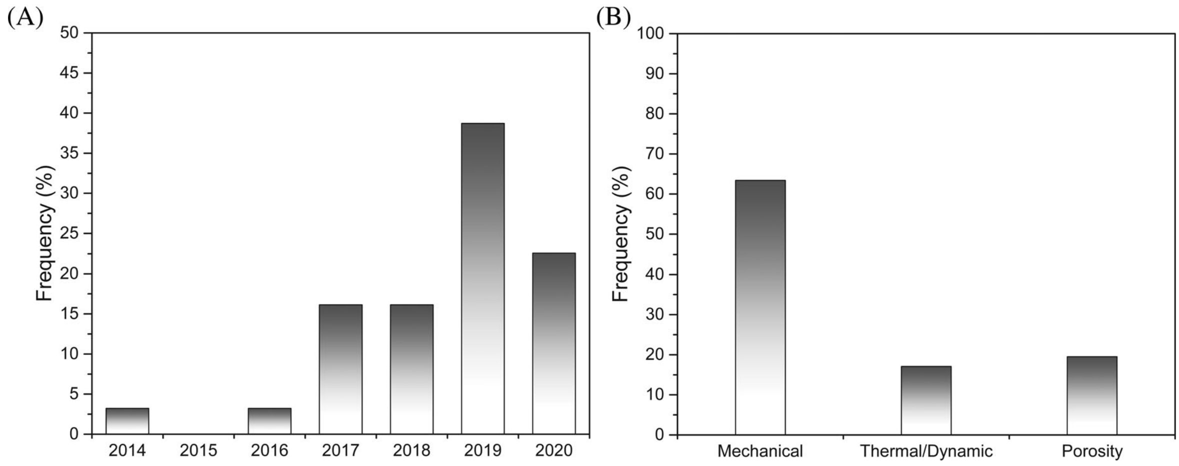

FIGURE 6 Frequency of (A) published papers per year and (B) test performed

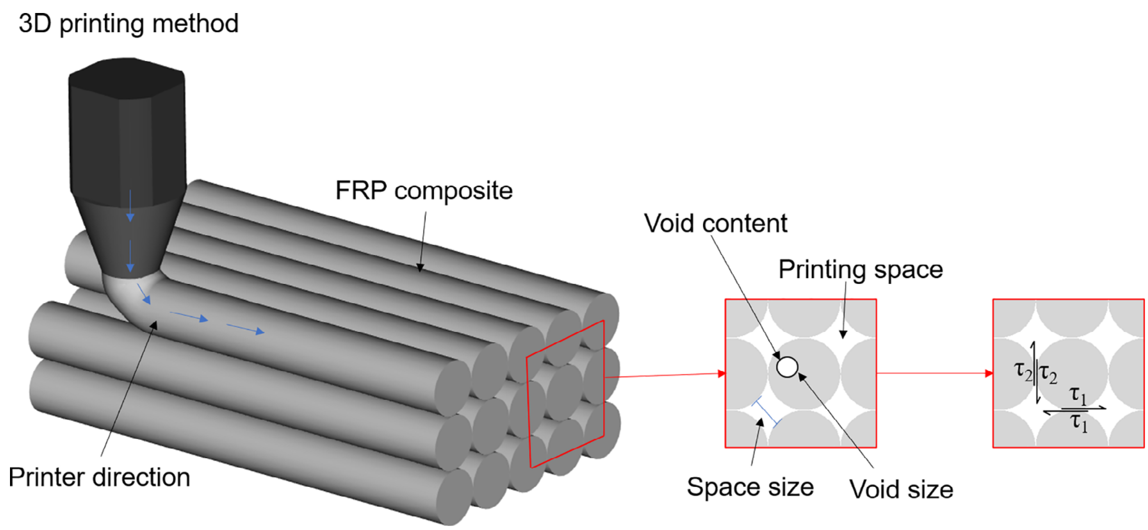

FIGURE 7 General schematic representation of void location and tension distribution in additive manufacturing [Color figure can be viewed at wileyonlinelibrary.com]

Figure 7 illustrates an additive manufacturing scheme, showing the printing direction, void content, and shear force distribution. One of the main factors that have to be controlled in AM is the void formation as well as for conventional composites.[34,42,43] However, the great difference for a AM composite is the free spacing generated between filaments, which reduces the contact area and generates lower shear and delamination resistance, as shown in Figure 7, decreasing the material mechanical properties.[44]

The void formation is directly proportional to processing parameters, but it is also affected by air trapped in the system and humidity.[27] The increase of printing speed, printing space, thickness, and inappropriate pressure and temperature are the main parameters to promote void formation.[16,17,34] The curing temperature of the polymer could also result in residual stress that eventually forms micro-cracks between the printing sections, promoting internal porosity.[7] Printing speed increases the deposited material density and reduces empty spaces, as illustrated by Ming et al.,[16] in which the porosity increases from 2% to 7% for speeds of 200–1400 mm.min^{-1}, respectively. The void morphology is also affected by processing parameters, in which the inclination and flattening of porosities occur due to shear resulted from infusion pressure and printing speed. Furthermore, the printing space increases the void fraction, in which the increase of the space within 1–1.4 mm generates an increase of 6%–17% in the void content.[16] The increase in fiber

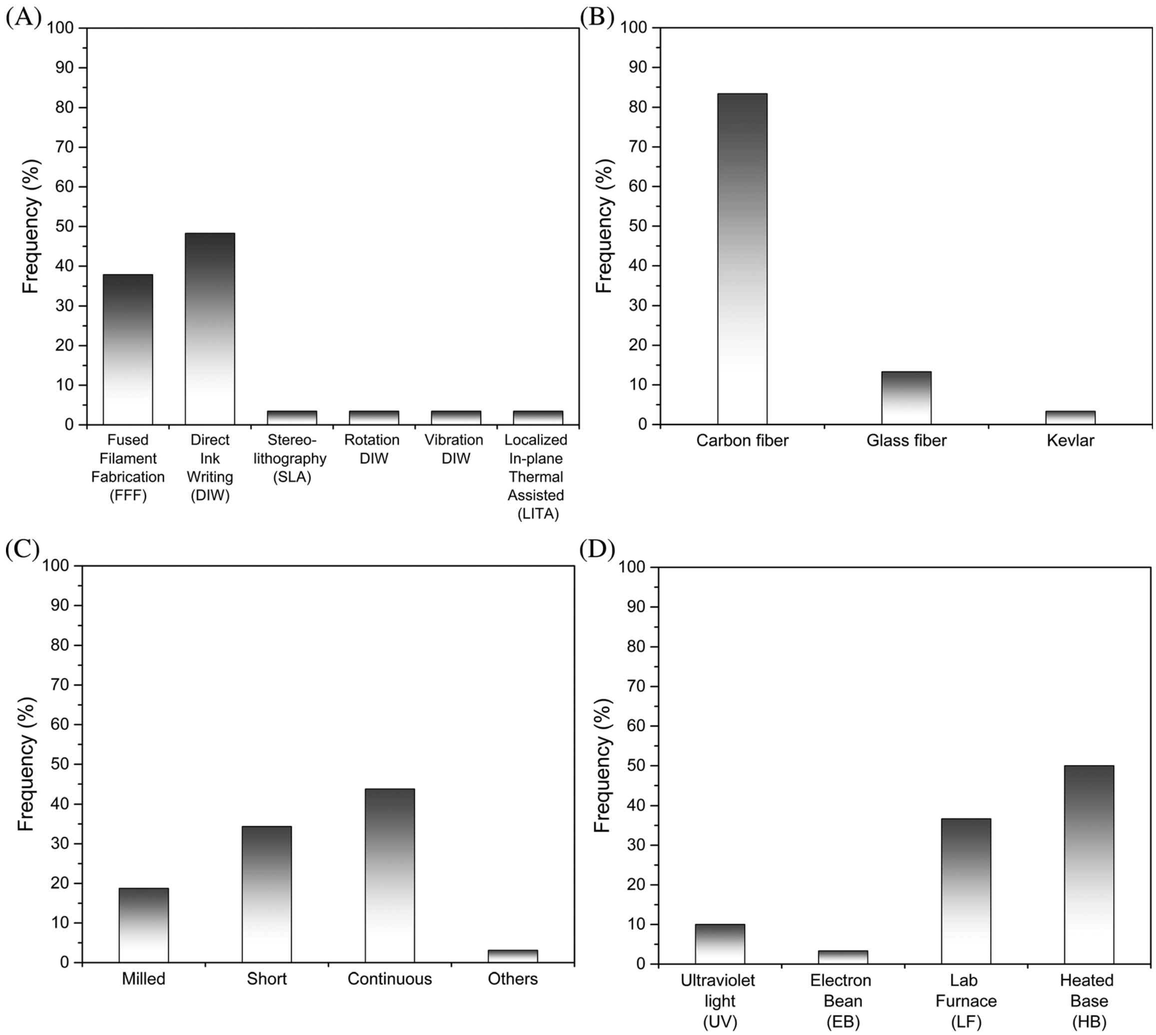

FIGURE 8 Frequency of (A) AM method, (B) fiber used, (C) fiber size, and (D) curing procedure

content also causes difficulty on the interfacial interaction due to agglomeration, increasing the void volume fraction.[34] These factors directly affect the mechanical properties of 3D printed parts.

Most AM methods used are FFF and DIW, as shown in Figure 8(A). In the FFF, the solid polymeric filament is melted and extruded through a nozzle. This method is widely used for continuous and discontinuous fibers. According to Nawafleh et al.,[34] the FFF limitation is associated with a large number and size of void formation through spaces between printed filaments, which reduces the mechanical performance caused by filament shearing and, therefore, may facilitate delamination. On the other hand, DIW presents no space between filaments, reducing the probability of void formation. However, this technique uses liquid polymer as the ink for a direct extruding from the nozzle, requiring short or miller fibers, reducing the mechanical properties.[34]

The SLA or vat photopolymerization technique uses ultraviolet (UV) light to control the temperature during injection, in which the composite processing accuracy is high as heat shrink ability is virtually absent. However, it is not much used since the epoxy curing needs to be UV-curable and needs a post-curing step.[36] The rotation and vibration in DIW are parameters that improve the processing, allowing an orientation controlling of short fibers by the nozzle rotation and vibrating integrated extrusion system for the possibility of higher reinforcement content use, respectively.[17,41]

The LITA printing enables a fast infusion and curing system for three-dimensional shapes through the impregnation and forming of continuous reinforcement with the epoxy system, following the capillary-driven concept.[12] Vibration/rotation DIW and LITA techniques are new and present no more than one study for each one (Figure 8(A)).

TABLE 1 Void analysis, mechanical, and thermal/dynamical mechanical tests performed for thermoset composites processed by different AM methods

				Testing		
References	**Matrix**	**Fiber**	**AM process**	**Void analysis**	**Mechanical tests**	**Thermal/dynamic mechanical**
[12]	Epoxy	Carbon: long	LITA	SEM: 0.465%	Tensile: X_t: 810 MPa E_t: 108 GPa	–
[16]	Epoxy	Carbon: long	FFF	SEM: 2–17%	Bending: X_f: 700–950 MPa E_f: 605–915 GPa E_f: 1.05–1.25% C: 0.15–2.6 N	–
[17]	Epoxy	Carbon: long and short	DIW	–	Bending: *Long fiber* X_f: 110–275 MPa E_f: 6–37 GPa *Short fiber* X_f: 75–150 MPa E_f: 4–9 GPa	–
[19]	Epoxy	Carbon: long	FFF	X-ray μCT: 2.53–7.02%	Bending: X_f: 360–400 MPa E_f: 18–22 GPa	–
[32]	Epoxy	Carbon: long	FFF	–	Bending: X_f: 375–410 MPa E_f: 16–17.5 GPa	–
[20]	Epoxy	Carbon: long	FFF	–	Bending: X_f: 60–112 MPa	–
[14]	Epoxy	Carbon: long	FFF	–	Bending: X_f: 616–861 MPa E_f: 51–72 GPa	–
[8]	Epoxy	Carbon: long	FFF	Density	Tensile: X_t: 4250–7737 N	–
[15]	Epoxy	Carbon: short	DIW	–	Blohm: L_m: 75–100 N/g δ: 1.15–1.65 mm *Two-hole clevis plate* L_m: 0.16–0.24 kN/g δ: 0.5–0.59 mm	–
[18]	Epoxy	Carbon: chopped	DIW	–	Tensile: X_t: 70–130 MPa	DMA: T_g: 132°C

TABLE 1 (Continued)

References	Matrix	Fiber	AM process	Testing		
				Void analysis	Mechanical tests	Thermal/dynamic mechanical
					E_t: 3.5–10.5 GPa Bending: X_f: 125–170 MPa E_f: 4.5–9.5 GPa	
[48]	Epoxy + PLA	Carbon: long	CFF	–	Bending: X_f: 38.9 MPa/kg E_f: 3325 GPa/kg	–
[9]	Epoxy	Carbon: long	DIW	SEM: 15%	–	DMA: T_g: 130°C E': 8.7 GPa TGA: 250°C
[44]	Epoxy	Carbon: long	FFF	OM: 2.53%	Tensile: X_t: 1476 MPa E_t: 100 GPaBending: X_f: 858 MPa E_f: 72 GPaShort beam: SBS: 49 MPa	–
[35]	Epoxy	Carbon: short	FDM	–	Tensile: X_t: 792 MPa E_t: 161 GPaBending: X_f: 202 MPa E_f: 144 GPa	–
[13]	Epoxy	Carbon: short	DIW	–	–	DMA: T_g: 120°C E': 3 GPa
[49]	Epoxy	Carbon: long	FDM	–	Bending: X_f: 693 MPa E_f: 59 GPa ε_f: 1.27%Charpy impact EA: 78 kJ/m^2	–
[50]	Epoxy	Carbon: short	DIW	–	Tensile: E_t: 57 GPa	–
[51]	Epoxy	Carbon: short	DIW	–	Tensile: X_t: 750 MPa E_t: 65 GPa	–

(Continues)

TABLE 1 (Continued)

References	Matrix	Fiber	AM process	Testing		
				Void analysis	Mechanical tests	Thermal/dynamic mechanical
[47]	Epoxy	Carbon: milled	DIW	–	–	DMA: E': 3.8–7.7 GPA Tan δ: 76–139°C
[31]	Epoxy	E-glass	DIW	–	Tensile: X_t: 272 MPa E_t: 8 GPa Bending: X_f: 299 MPa E_f: 6 GPaShort beam: *SBS*: 34 MPa	–
[30]	Phenol formaldehyde	E-glass	DIW	OM: 5.3–5.8%	Tensile test X_t (MPa): 86–96 Bending test X_f (MPa): 119–137	–
[52]	Epoxy	E-glass	DIW	–	Tensile: X_t: 3–11 MPa E_t: 2–6 GPa	DSC: 1.23 kJ/kg K Thermal conductivity: 0.65 W/m K
[34]	Epoxy	Aramid: short	DIW	OM: 1.39–12.04%	Bending: X_f: 52–108 MPa E_f: 3.2–4.2 GPa ε_f: 1.2–0.8%Fatigue: 10^6 cycles: 24–37 MPa	DMA: E': 160–300 kPa
[45]	Epoxy	Carbon: short	DIW	–	Tensile: X_t: 0.08–0.14 MPa E_t: 35–5.5 GPa ε_t: 6–22%	–
[53]	Epoxy	Carbon: short	FDM	–	Shore D Hardness: 89.8	–
[46]	Epoxy	Carbon: long	FFF	–	Tensile: X_t: 34–37 MPaE_t: 4.8–5.1 GPa	–
[41]	Epoxy	Carbon: short	DIW	–	Compression: *EA*: 249–490 mJ P_f: 226–321 N I_s: 432–812 N/mm δ: 1.81–2.27 mm	–

TABLE 1 (Continued)

References	Matrix	Fiber	AM process	Testing		
				Void analysis	Mechanical tests	Thermal/dynamic mechanical
[37]	Epoxy	Carbon: short	DIW	–	Tensile: E_t: 8–11 GPaX_t: 66–97 MPa	DMA: E': 700 kPa
[36]	Epoxy	E-glass	Stereolithography (SLA)	–	Tensile test X_t: 15–80 MPaE_t: 0.2–1.8 GPa	–

Abbreviations: DIW, 3D vibration direct ink writing; E', storage modulus; EA, energy absorption; E_f, bending modulus; E_t, tensile modulus; I_s, initial stiffness; L_m, load/mass; P_f, peak force; SBS, short bean strength; X_f, bending strength; X_t, tensile strength; δ, displacement; ε_f, bending strain; ε_t, tensile strain; C, compaction force; CFM, composite filament fabrication; DSC, differential scanning calorimetry; DMA, dynamic mechanical analysis; FFF, fused filament fabrication; FDM, fused deposition modeling; OM, optical microscopy; LITA, localized in-plane thermal assisted printing; PLA, polylactide.

Carbon fibers are the most used reinforcement in AM, mainly given their high mechanical properties (Figure 8(B)). The high interaction of carbon fibers and the epoxy system is a second factor for high use as the main reinforcement.[18,45] Following Nawafleh et al.,[34] short aramid fiber presents a significant increase in mechanical performance compared with neat resin. However, with lower mechanical (3-point bending and tension) and dynamical mechanical (storage modulus) properties than carbon fiber. Glass fiber is less used. However, considering their lower price, it could be an alternative for experimental optimization of the AM process.

The most used type of fiber is the continuous one due to its high mechanical performance. Short and milled fibers are also utilized at a lower frequency, based on the ease of processing with shorter fibers, generating lower mechanical and dynamic properties.[17] The other fiber size is cut in non-determined size,[46] presenting an intermediate properties response between short and continuous fiber (more prone to short fiber property).

Finally, the most common processing methods for temperature control are the heated base–usually used for AM technique,[47] and lab furnace–procedure to cure the specimen in a furnace after printed injection.[13,29] The UV-assisted cure system uses light to control temperature during injection and curing, which is less used, but with greater efficiency.[33,36] Electron beam-induced radiation curing uses accelerated electrons to provide energy for the initial cure process by decomposing a radiation-sensitive initiator, which is a fast and accurate cure procedure. Nevertheless, it is challenging to incorporate the entire thickness, mainly for larger components.[32]

Table 1 lists the 29 results of the thermoset composite processed by AM studies following PRISMA systematic search terms used in the present method (Figure 5). The reinforcement used (carbon fiber, glass fiber, Kevlar) and AM are also provided in Table 1 with the respective characterization (void content, mechanical, thermal, and dynamical mechanical). Full detail for each study listed in Table 1 can be found in Table S1 in the supplementary material.

Regarding mechanical results, it is difficult to establish a direct comparison between the reinforcement types used so far since each published research paper presents studies with distinct fiber volume fraction, processing type, and used test. Nevertheless, their mechanical properties follow this sequence: carbon fiber > aramid fiber > glass fiber. This means that the overall mechanical performance of the composite is directly associated with the mechanical behavior and interfacial adhesion of each fiber.

With the use of milled fibers, higher reinforcement fraction can take place (up to 80% for glass fiber[30]), increasing the composite mechanical performance. Aramid fibers present only up to 6.3% of short fiber volume fraction, however, having higher bending strength and fatigue life.[34] Continuous fibers have greater loading capacity due to better load distribution. The study showed that higher fiber volume fraction for continuous carbon fiber (i.e., 58%) was achieved with LITA processing.[37]

The bonding analysis for AM is divided into two main aspects: fiber/matrix interfacial bonding and imprinting filament bonding. The first bonding (between fiber/matrix) depends on fiber and matrix surface nature and fiber treatment. The covalent bonding and growth pattern of carbon fiber/epoxy and glass fiber/epoxy exhibits high conductivity, strength, and modulus along the fiber direction.[19] The higher mechanical performance for short aramid fibers is due to the strong adhesion and wetting between aramid and epoxy matrix, even for low fiber volume fractions.[34] Li et al.[30] show that alkaline glass fiber treatment adsorbs water vapor, dust, and other substances, reduces the bonding effect between glass fiber/matrix, and reduces the mechanical strength of the composite. The second (filament bonding) is governed by processing parameters and matrix bonding features, in which printing speed, space, thickness, curing pressure, and temperature control the bonding between adjacent print filament and avoid gap and other defects of printed parts.[14,16] The interfacial adhesion optimization between printed layers is the focus that needs improvement in AM applications to ensure high delamination and shear strength for the material.[54]

The matrix system is of great interest for additive manufacturing, mainly for thermoset matrices, since this phase strongly influences the processing control (part dimensional tolerance, interfacial adhesion, curing parameters, among others).[16,38] The matrix choice and processing parameters must be strictly controlled to ensure the printing with low defect formation at the matrix/fiber interface and guarantee the adhesion between printed layers, considering that the latter has been a great challenge for improving AM processes. Several works in this review used bi-component epoxy resin given its advantages in terms of viscosity and curing control following the resin to hardener ratio, expanding the operational control of the process. The most widely used bi-component resins are DER 671/661 and EPON 826 types, as they present low viscosity, high-strength, and mainly due to low curing temperature, an essential factor for processing control via additive manufacturing.[14,32,38,55]

6 | CONCLUSIONS

A systematic review was performed here focusing on FRP thermoset composite processed by additive manufacturing in the time range of 2014–2020. The AM method and type of reinforcement were included, focusing on void content, mechanical, and thermal/dynamic mechanical properties. The systematic review proved to be a useful tool for easily indicating the trends and lacks in the searched topic. In addition, the current work provides a reference document for future research. Considering the novelty, the main literature gap is the absence of the void formation control studies, directly influencing the material properties. This control will be even more critical in more complex geometries than most of the works presented. In addition, the most used processes are those already used for thermoplastic composites. The newer processes (vibration and rotation of DIW) have already shown improvements in mechanical properties, exhibiting the need for a more appropriate AM method for thermoset matrices capable of reducing defects formation (e.g., voids) and ensuring processing various fibrous reinforcement types. The interfacial adhesion optimization between printed layers is the focus that needs improvement in AM applications to ensure high delamination strength for the material. As a matter of fact, there is a low number of thermal and dynamic tests, which are also relevant for the related materials processed by AM, considering that the thermal process control, void formation, and printing direction characteristics can modify their dynamic behavior, long-term performance (creep/recovery), among others. Considering that milled, chopped, or short fibers are usually used, the possibility of using reclaimed reinforcing fibers is important for environmental aspects, which is not yet explored.

7 | FUTURE PERSPECTIVES

Thermoset polymers exhibit superior thermal, chemical, and mechanical stability compared to most thermoplastic matrices, making them ideal for structural applications. Nevertheless, thermoset polymer processing typically requires molds and complex/heavy tooling. This makes it a challenge to fabricate complex architectures, and the customized manufacturing assembly are costly. AM is a promising way to overcome these issues. AM composites present unique hierarchical porous structures with extensive micron-sized pores, which are uncommon in typical 3D typical parts, but highly desired in various applications, including tissue engineering scaffolds, sensors, and actuators–

associated with their lightweight, high surface area, and efficient mass transportation.

Some negative impacts include health hazards (additive manufacturing can emit up to 200 billion tiny toxic particles per minute and, when inhaled, can penetrate our lungs, cause irritation), and eco-unfriendly (most printers use plastic filaments), and high energy consumption.

ACKNOWLEDGMENTS

Francisco M. Monticeli thanks FAPESP (process number: 2017/10606-4); Roberta M. Neves acknowledges CAPES (financial code 001); and José Humberto S. Almeida Jr is supported by the Royal Academy of Engineering under the Research Fellowship scheme (Grant No. RF/201920/19/150).

ORCID

Francisco M. Monticeli https://orcid.org/0000-0002-0814-8160
Roberta M. Neves https://orcid.org/0000-0002-7017-0852
Heitor L. Ornaghi Jr https://orcid.org/0000-0002-0005-9534
José Humberto S. Almeida Jr https://orcid.org/0000-0002-9408-7674

REFERENCES

[1] G. Belingardi, M. P. Cavatorta, *Int. J. Fatigue* **2006**, *28*, 815.
[2] J. M. Reverte, M. Caminero, J. M. Chacón, E. García-Plaza, P. J. Núñez, J. P. Becar, *Materials* **2020**, *13*, 1924.
[3] X. Tian, T. Liu, C. Yang, Q. Wang, D. Li, *Compos Part A Appl. Sci. Manuf.* **2016**, *88*, 198.
[4] K. A. Evans, Z. C. Kennedy, B. W. Arey, J. F. Christ, H. T. Schaef, S. K. Nune, et al., *ACS Appl. Mater. Interfaces* **2018**, *10*, 15112.
[5] J. F. Christ, N. Aliheidari, A. Ameli, P. Pötschke, *Mater. Des.* **2017**, *131*, 394.
[6] M. A. Caminero, J. M. Chacón, I. García-Moreno, J. M. Reverte, *Polym. Test.* **2018**, *68*, 415.
[7] N. Van de Werken, P. Koirala, J. Ghorbani, D. Doyle, M. Tehrani, *Addit. Manuf.* **2021**, *37*, 101634.
[8] H. J. Kim, H. S. Kim, G. Y. Lee, M. S. Kim, S. H. Min, R. Keller, et al., *Compos. Part B Eng.* **2019**, *174*, 106945.
[9] S. Mishra, P. Katti, S. Kumar, S. Bose, *Chem. Eng. J.* **2019**, *357*, 384.
[10] O. Uitz, P. Koirala, M. Tehrani, C. C. Seepersad, *Addit. Manuf.* **2021**, *41*, 101919.
[11] A. Abbott, T. Gibson, G. P. Tandon, L. Hu, R. Avakian, J. Baur, et al., *Addit. Manuf.* **2021**, *37*, 101636.
[12] B. Shi, Y. Shang, P. Zhang, A. P. Cuadros, J. Qu, B. Sun, et al., *Matter* **2020**, *2*, 1594.
[13] N. Nguyen, E. Melamed, J. G. Park, S. Zhang, A. Hao, R. Liang, *Macromol. Mater. Eng.* **2017**, *302*, 1.
[14] H. Xiao, W. Han, Y. Ming, Z. Ding, Y. Duan, *Materials (Basel)* **2019**, *6*, 23058.
[15] f. W. S. Fernandez, J. P. Compel, D. A. Lewicki, *Tortorelli, Comput. Methods Appl. Mech. Eng.* **2019**, *353*, 277.
[16] Y. Ming, S. Zhang, W. Han, B. Wang, Y. Duan, H. Xiao, *Addit. Manuf.* **2020**, *33*, 101184.
[17] N. Nawafleh, E. Celik, *Addit. Manuf.* **2020**, *33*, 101109.
[18] H. A. Pierson, E. Celik, A. Abbott, H. de Jarnette, L. Sierra Gutierrez, K. Johnson, et al., *Exp. Mech.* **2019**, *59*, 843.
[19] Y. Ming, Y. Duan, S. Zhang, Y. Zhu, B. Wang, *Polym. Test.* **2020**, *82*, 106309.
[20] J. F. P. Lovo, I. L. de Camargo, L. A. O. Araujo, C. A. Fortulan, *Proc. Inst. Mech. Eng. Part. C J. Mech. Eng. Sci.* **2020**, *234*, 417.
[21] C. di Fratta, F. Klunker, F. Trochu, P. Ermanni, *Compos. Part A Appl. Sci. Manuf.* **2015**, *77*, 238.
[22] M. Li, S. K. Wang, Y. Z. Gu, Y. X. Li, K. Potter, Z. G. Zhang, *Compos. Sci. Technol.* **2012**, *72*, 873.
[23] F. M. Monticeli, D. C. Monte Vidal, M. Y. Shiino, H. J. C. Voorwald, M. O. H. Cioffi, *Polym Eng Sci* **2019**, *59*, 1215.
[24] A. Yudhanto, M. Almulhim, F. Kamal, R. Tao, L. Fatta, M. Alfano, et al., *Compos. Sci. Technol.* **2020**, *199*, 108346.
[25] A. Liberati, D. G. Altman, J. Tetzlaff, C. Mulrow, P. C. Gøtzsche, J.P.A. Ioannidis JPA, et al., *J. Clin. Epidemiol.* **2009**, *62*, 1.
[26] R. M. Neves, L. H. Ornaghi Jr.., A. J. Zattera, S. C. Amico, *Carbohydr. Polym.* **2020**, *255*, 117366.
[27] S. H. R. Sanei, D. Popescu, *J. Compos. Sci.* **2020**, *4*, 98.
[28] A. P. O. Costa, A. E. Gerbase, C. L. Petzhold, *Polimeros* **2011**, *21*, 146.
[29] S. Vyazovkin, A. K. Burnham, J. M. Criado, L. A. Pérez-Maqueda, C. Popescu, N. Sbirrazzuoli, *Thermochim. Acta* **2011**, *520*, 1.
[30] Z. Li, W. Zhou, L. Yang, P. Chen, C. Yan, C. Cai, et al., *Polymers (Basel)* **2019**, *11*, 135.
[31] Y. Ming, Z. Xin, J. Zhang, Y. Duan, B. Wang, *Compos. Commun.* **2020**, *21*, 100401.
[32] B. Wang, Y. Ming, Y. Zhu, X. Yao, G. Ziegmann, H. Xiao, et al., *Addit. Manuf.* **2020**, *31*, 100967.
[33] H. Sun, Y. Kim, Y. C. Kim, I. K. Park, J. Suhr, D. Byun, et al., *J. Mater. Chem. C* **2018**, *6*, 2996.
[34] N. Nawafleh, F. K. E. Elibol, M. Aljaghtham, E. Oflaz, A. J. Ciciriello, C. M. Dumont, et al., *J. Mater. Sci.* **2020**, *55*, 11284.
[35] W. Hao, Y. Liu, H. Zhou, H. Chen, D. Fang, *Polym. Test.* **2018**, *65*, 29.
[36] Y. Sano, R. Matsuzaki, M. Ueda, A. Todoroki, Y. Hirano, *Addit. Manuf.* **2018**, *24*, 521.
[37] B. G. Compton, J. A. Lewis, *Adv. Mater.* **2014**, *26*, 5930.
[38] K. J. Johnson, L. Wiegart, A. C. Abbott, E. B. Johnson, J. W. Baur, H. Koerner, *Langmuir* **2019**, *35*, 8758.
[39] N. Van de Werken, H. Takinalp, P. Khanbolouki, S. Ozcan, A. Williams, M. Tehrani, *Additiv. Manuf.* **2020**, *31*, 100962.
[40] R. Matsuzaki, M. Ueda, M. Namiki, T. K. Jeong, H. Asahara, K. Horiguchi, et al., *Sci. Rep.* **2016**, *6*, 1.
[41] J. R. Raney, B. G. Compton, J. Mueller, T. J. Ober, K. Shea, J. A. Lewis, *Proc. Natl. Acad. Sci. U. S. A.* **2018**, *115*, 1198.
[42] Y. K. Hamidi, L. Aktas, M. C. Altan, *Compos. Sci. Technol.* **2005**, *65*, 1306.
[43] F. M. Monticeli, H. L. Ornaghi, H. J. Cornelis Voorwald, M. O. H. Cioffi, *Compos Part A Appl Sci Manuf* **2019**, *125C*, 105555.

[44] Y. Ming, Y. Duan, B. Wang, H. Xiao, X. Zhang, *Materials (Basel)* **2019**, *12*, 1369.
[45] J. P. Lewicki, J. N. Rodriguez, C. Zhu, M. A. Worsley, A. S. Wu, Y. Kanarska, et al., *Sci. Rep.* **2017**, *7*, 1.
[46] A. S. Ramírez, R. d'Amato, F. B. Haro, M. I. Marcos, J. A. Juanes, *J. Med. Sys.* **2019**, *43*, 120.
[47] G. Griffini, M. Invernizzi, M. Levi, G. Natale, G. Postiglione, S. Turri, *Polymer* **2016**, *91*, 174.
[48] A. V. Azarov, F. K. Antonov, M. V. Golubev, A. R. Khaziev, S. A. Ushanov, *Compos. Part B Eng.* **2019**, *169*, 157.
[49] G. Szebényi, T. Czigány, B. Magyar, J. Karger-Kocsis, *Express Polym. Lett.* **2017**, *11*, 525.
[50] S. Malek, J. R. Raney, J. A. Lewis, L. J. Gibson, *Bioinspir. Biomim.* **2017**, *12*, 026014.
[51] A. V. Azarov, F. K. Antonov, V. V. Vasil'ev, M. V. Golubev, D. S. Krasovskii, A. F. Razin, et al., *Polym. Sci. – Ser. D* **2017**, *10*, 87.
[52] B. L. Tai, Y. T. Kao, N. Payne, Y. Zheng, L. Chen, A. J. Shih, *Med. Eng. Phys.* **2018**, *61*, 61.
[53] E. R. Griffiths, S. J. Leigh, *Sensors Actuators A Phys.* **2019**, *296*, 272.
[54] P. Parandoush, D. Lin, *Compos. Struct.* **2017**, *182*, 36.
[55] K. D. Jones, A. T. Dibenedetto, *Compos Sci Technol* **1994**, *51*, 53.

SUPPORTING INFORMATION

Additional supporting information may be found online in the Supporting Information section at the end of this article.

How to cite this article: F. M. Monticeli, R. M. Neves, H. L. Ornaghi Jr, J. H. S. Almeida Jr, *Polymer Composites* **2021**, 1. https://doi.org/10.1002/pc.26133